A new force-feedback arm exoskeleton for haptic interaction in Virtual Environments

A. Frisoli F. Rocchi S. Marcheschi A. Dettori F. Salsedo M. Bergamasco
PERCRO Scuola Superiore S. Anna, Italy
E-mail contact author: antony@sssup.it

Abstract

The paper presents the mechanical design of the L-EXOS, a new exoskeleton for the human arm. The exoskeleton is a tendon driven wearable haptic interface with 5 dof, 4 actuated ones, and is characterized by a workspace very close to the one of the human arm. The design has been optimized to obtain a solution with reduced mass and high stiffness, by employing special mechanical components and carbon fiber structural parts. The devised exoskeleton is very effective for simulating the touch by hand of large objects or the manipulation within the whole workspace of the arm. The main features of the first prototype that has been developed at PERCRO *are presented, together with an indication of the achieved and tested performance.*

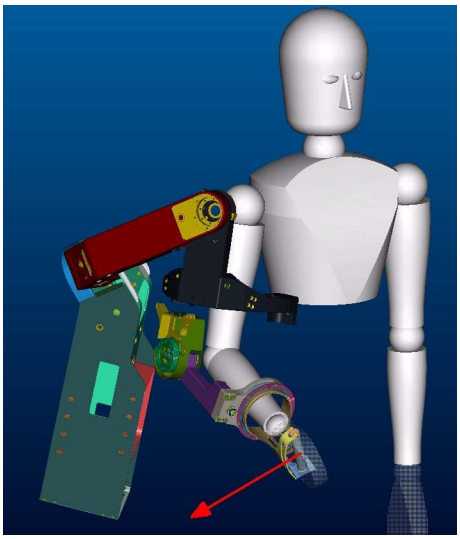

Figure 1. The arm exoskeleton

1. Introduction

L-EXOS (Light Exoskeleton) [12] is an exoskeleton based haptic interface for the human arm. The L-Exos has been designed as a wearable haptic interface, capable of providing a controllable force at the center of user's right-hand palm (Figure 1), oriented along any direction of the space. It is a 5 dof robotic device with a serial kinematics, isomorphic to the the human arm. It is suitable for application where both motion tracking and force feedback are required, such as human interaction with virtual environments or teleoperation/telemanipuation tasks. Exoskeletons [1] [2] [3] can bring up a valuable contribution to the applications where the workspace is strategic. In CAVE-like environments exoskeletons can minimize the visual interference [4] with virtual objects; in rehabilitation or in simulation of industrial assembling and maintenance operations they can provide large workspace, complex force information (both force and torques) and higher number of contact points.

Two configurations of the device have been conceived:

C1 In the configuration C1 (L-EXOS), an handle is mounted on the last link and the system is composed of 5 dof, of which 4 actuated ones only. The non actuated degree of freedom is the last one, aligned along the anatomical prono-supination axis of the forearm (Figure 1).

C2 In the configuration C2, the non-actuated degree of freedom and the handle are replaced with an hand-exoskeleton that can apply generic force on two fingertips of the right hand, preferably thumb and index fingers, as shown in Figure 2.

The configuration C2 is particularly innovative, since it can reach up to three contact points, one located on the palm/forearm of the user, and the other two ones directly on the fingertips of the hand. This paper will focus in particular on the mechanical design and the performance of the exoskeleton in its configuration C1.

Proceedings of the First Joint Eurohaptics Conference and Symposium on Haptic Interfaces for Virtual Environment and Teleoperator Systems
0-7695-2310-2/05 $20.00 © 2005 **IEEE**

Figure 2. The arm exoskeleton integrated in its configuration C2

2. Kinematics and user's requirements

L-exos is characterized by a serial kinematics consisting of five rotational joints (see Figure 3) of which the first four ones are actuated and sensorized, while the last one is only sensorized.

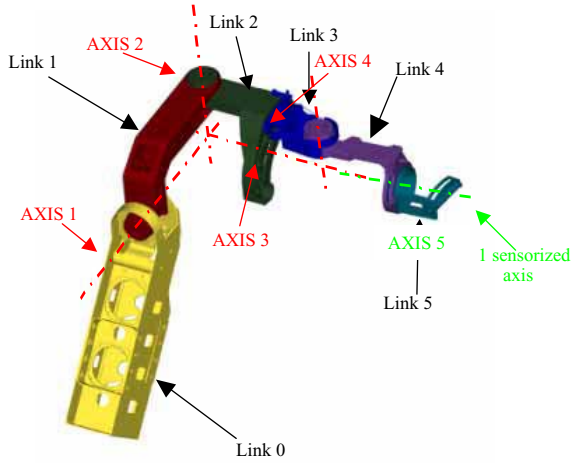

Figure 3. The general kinematics of the L-Exos

The first three rotational axes are incident and mutually orthogonal (two by two) in order to emulate the kinematics of a spherical joint with the same center of rotation of the human shoulder. The target workspace for the shoulder joint was assumed to be the quadrant of a sphere, as shown in Figure 4.

The orientation of the first axis was optimized to maximize the workspace of the shoulder joint, by avoiding singularities and interferences between the mechanical links and the operator. The optimization process provided also indications for the definition of the shapes of the links. As a result from the kinematic analysis, the final orientation of the first axis (the fixed one) was chosen to be skewed with respect to the horizontal and vertical plane, while the third axis was assumed to be coincident with the ideal axis of the upper arm. This implied that the third joint had to be implemented with a rotational pair aligned with the forearm.

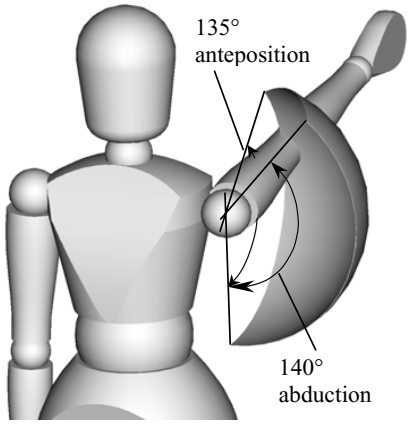

Figure 4. The reachable workspace of the arm exoskeleton

The fourth axis was assumed coincident with the elbow joint and the fifth axis with the forearm, in order to allow the prono-supination of the wrist.

The workspace of the elbow coincides with the angle of rotation of the fourth axis. Assuming the position of zero when the forearm and the arm are aligned, the range of motion achieved by the L-Exos spans approximately from 2.5 to 105 degrees. The wrist has only 1 non actuated dof, and its range of motion is of 180°, and precisely $\pm 90°$ measured when the hand palm is aligned with arm and forearm in the zero position.

3. Mechanical Design

3.1. Design guidelines

In order to improve the transparency of use of the device, a set of guidelines have been adopted for the mechanical design:

- Remote placement of motors: this allows to drastically reduce the perceived inertia (increase of inter-

face transparency) and the joint torque required for the gravitational compensation, and so the motors size and the transmissions tension;

- Selection of motors with high torque to weight ratio;
- Use of tendon transmissions: even though they have low stiffness, they can easily transmit torques to joints placed far apart from motors with zero backlash, low friction and low weight;
- Low transmission ratio: this allows to reduce the contribution of the motors to the perceived inertia at the end-effector and so to lower the perceived transmission friction;
- Low or zero backlash implementation of the joints;
- Use of light materials for the construction of the moving parts;
- Guarantee of a safe, comfortable and ergonomic use of device.

4. Mechanical Constructive Features

All the motors of the exoskeleton have been located on the fixed frame (Link 0). For each actuated DOF, the torque is delivered from the motor to the corresponding joint by means of steel cables and a reduction gear integrated at the joint axis, as can be seen from the scheme of the transmission of axis 2 in Figure 5. Such an arrangement allows to reduce the masses of the moving parts, by reducing the mass of the motors (near 40% of the overall mass of the exoskeleton) and the additional mass of the structural parts, to be reinforced in order to sustain the weight of heavier motors. The inertia perceived by the user at the palm is also consequently reduced. The electric actuators offering the best torque to weight and torque to volume ratio have been selected.

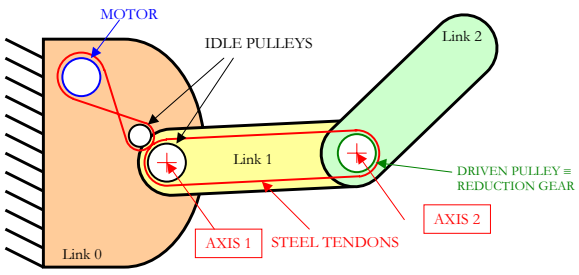

Figure 5. Scheme of the actuation of the joint 2.

In order to ground the motors long transmissions were required. They have been implemented through steel cables that can guarantee low weight and zero backlash, even if presenting low mechanical stiffness. Moreover cable transmissions are more efficient than gear transmissions, thus ensuring a better grade of backdrivability of the system.

To achieve a higher stiffness of the device at the end effector, reduction gears with low reduction ratio were located at the joint axes, thus allowing to reduce the tendon tensions, their elongation and their diameter. The reduction of the tendon diameter led to a consequent saving of mass and volume of all the mechanical parts of the transmission system (pulleys, axles, etc). Thanks to this solution and to the development of expressly conceived speed reducers (see section 5.2) a mass reduction of about 35% for the transmission system and of 40% for the structural parts has been achieved. The structural components (links) have been designed as thin-wall parts, that can house the mechanical parts of the transmission (pulleys, tendons, axles, spacers, etc) within the links, protecting the inner parts from external interference and the user from potential harm deriving by the tensed steel cables.

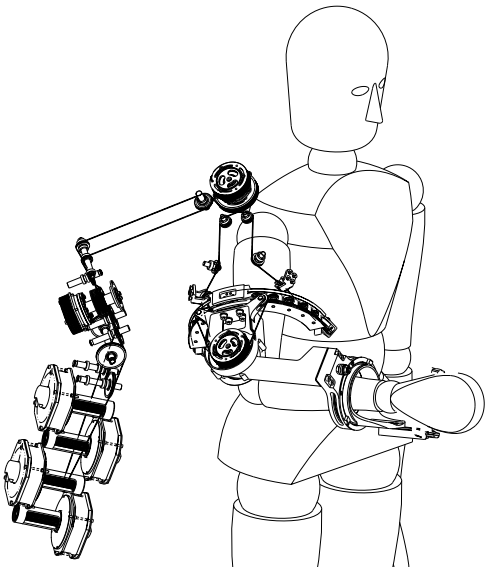

Figure 6. CAD model of the transmission system

Hollow sections, presenting a larger moment of inertia than bulk sections with the same area, were used to enhance the stiffness of the thin-wall parts. In order to further improve lightness and stiffness, the structural components were made of carbon fiber. Also aluminum parts were bonded on the carbon fiber structure to realize the connections with other mechanical components.

The carbon fiber parts were manufactured with the vacuum-bag technique, and with dies made of carbon

Figure 7. Example of a link and its die made of carbon fiber

fiber too (see Figure 7), due to the low number of prototypes manufactured (only 2). The carbon fiber used for the structural parts is the M46J (Torayca).

5. Special components

The mechanical design included some special components that were developed at PERCRO since no off the shelf component were found with the requested performance. Custom designed components not only can match the required performances, but also can be designed to be highly integrated with the remaining mechanical parts. Notwithstanding the high level of customization of these special components, they can be easily adapted to other devices, so that they can be considered as stand alone general-purpose devices. The developed components are: the Circular guide, the Integrated Planetary Reduction Gear and the Motor-Group.

5.1. Circular guide

The Circular Guide (Figure 8) [13] is a special component specifically developed for the implementation of the rotational joint of the L-EXOS. Since the joint 3 is aligned with the axis of rotation of the human arm, a Remote Center of Rotation was needed. The solution of adopting a closed circular bearing was replaced with an open circular one, based on recirculating ball bearings technology. This innovative solution allows the user to insert (and remove) the arm easily, with no need of inserting the arm through a closed-ring structure, so performing uncomfortable maneuvers.

With respect to the closed bearings, the Circular Guide presents two main advantages:

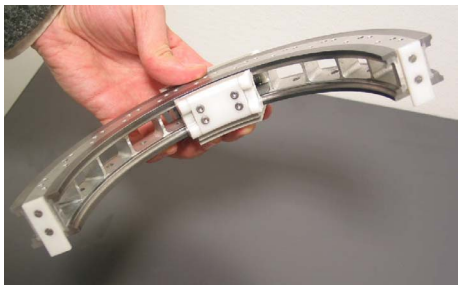

Figure 8. The open circular guide

- Higher achievable mobility of the shoulder during the abduction-adduction movement due to the elimination of the internal bulk of the component that limits the approaching of the user's arm to his trunk
- Easiness of wearing/unwearing

The Circular Guide is mainly composed by a fixed part with a open circular geometry (railway) and a mobile part (cursor). These two elements are made of aluminum alloy. The lift of the cursor is realized by 4 rolling tracks made of steel AISI 404.

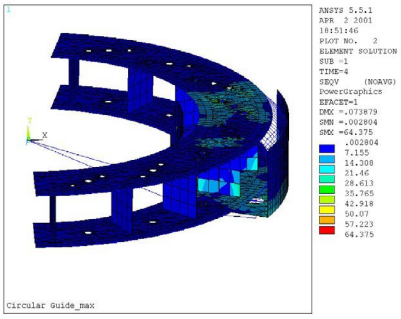

Figure 9. The FEM verification of the circular guide

The design of the component has been carried out with the target of minimizing the weight keeping unchanged the stiffness performances required for the particular application. The values of the main parameters like dimensions, balls number and the sensitivity of the component performance to the parameters change have been computed with a semiautomatic optimization procedure based on finite element analysis (Figure 9).

In the coordinate system of Figure 9, the following performance were finally achieved by the component:

Max Load:	50 N in x,y and z directions
Max Moments:	$M_x = M_z = 20$ Nm
Stiffness:	$C_x = C_y = C_z = 200$ N/mm ;
	$R_z = R_x = 8000$ Nm/rad

Weight: 0,6 Kg

5.2. The Joint-Integrated Planetary Reduction Gear

The reduction gear is the last element of the actuation system and is located on the joint axis. The primary target that was addressed during the design of the gearhead unit was the reduction of weight and volume with respect to standard commercial reduction gears. To fully pursue this target a high level of integration with the axis joint has been addressed.

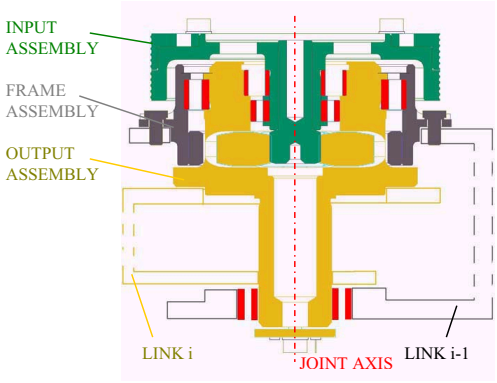

Figure 10. The integrated reduction gear

The number of parts has been reduced by requiring to the gearhead to accomplish multiple functions, beside of being a speed reduction unit only : the input shaft serves also as driven pulley of the transmission, while the output shaft is also the axle of each joint (see Figure 10). The interposition of the reduction gearhead between the tendon transmissions and the driven joint has led also to an enhancement of the stiffness of the system, by reducing the tension of the steel cables composing the transmissions.

The outstanding lightness is achieved partially by means of the aforementioned integration, but mostly by means of a design effort that allowed to use light alloy (aluminum alloy) instead of steel. The only parts of steel, apart from bolts and bearings, are the standard gears. A great effort has also been carried out to maintain the backlash introduced by the gears within a tolerable value. A lower value would imply a dramatic increase of the friction factor.

The main characteristics of the integrated gearhead are reported below for two different models that have been constructed:

Reduction ratio:	4/6
Mass (g)	345 / 360
D (mm)	73
L (mm - without axis)	42
Backlash (arcmin - output)	< 8
Efficiency	0.93

Figure 11. The integrated reduction gear

5.3. Motor Group

The four degrees of freedom are actuated by four identical motor groups. Each motor group is equipped with a frameless DC Permanent Magnet Torque Motor (VERNITRON 3730) and a high resolution optical encoder (1024 slots). In the motor group the driving pulley of the tendon drive is also included. The rotor of the motor is directly bonded on the driving pulley at its end side. The driving pulley is supported by two ball bearings located in correspondence of the two walls of the grounded link (link 0). The housing of the dc motor is cantilevered. All the structural parts of the motor group are made of lightweight alloy (Ergal 7075).

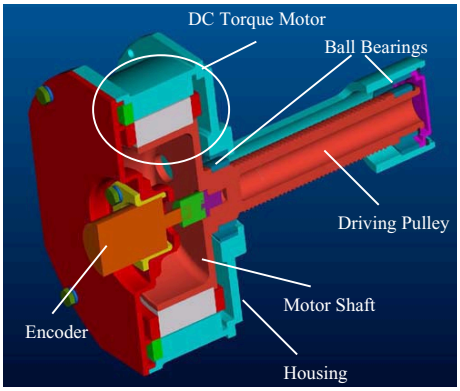

Figure 12. Scheme of the motorization group

0-7695-2310-2/05 $20.00 © 2005 **IEEE**

6. Performance of the integrated system

The L-EXOS, shown in Figure 13, can attain very remarkable performance, that can be summarized as follows:

Force	50 N continuous, 100 N peak force;
Backlash	10 mm at the end effector;
Stiffness	Estimated 3 N/mm, measured 2 N/mm;
Workspace	approximately 70% of that of human arm.

The L-Exos has a weight of 11 kg, of which approximately 6 kg distributed on the link 0, i.e. the fixed part, and mostly due to the mass of the 4 motor-groups. This means the L-EXOS achieve the desirable very low value of weight /payload ratio of almost 1 (100N vs. 11 Kg). The reported valued of stiffness of 3 N/mm represent the theoretical worst-case condition. The experimental measurements have provided a good confirmation of this value, even if the perceived stiffness seems to be amplified by the backlash introduced by the joint gearheads.

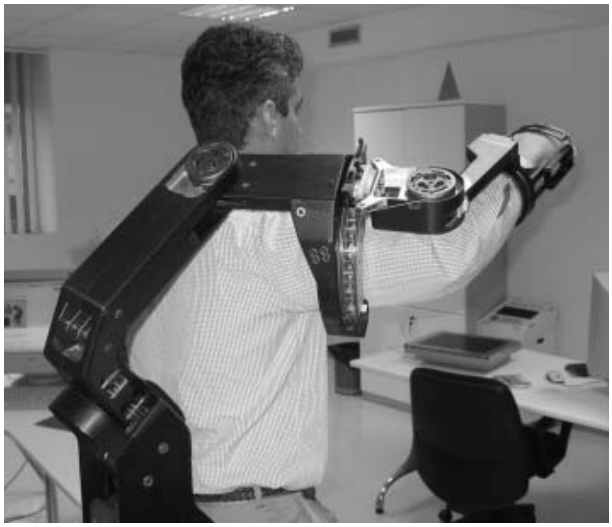

Figure 13. Pure-Forme exoskeleton.

7. Modeling and Control

7.1. Control architecture

The Control Unit provides the required real time support for running a Real Time operating system. It is based on a rackmount industrial PC with a Single Board Computer (SBC) with a 2.4GHz PENTIUM IV which provides the required computing power for a 2Khz control frequency. Inside the unit are also placed two 8 axis I/O boards, capable of managing required I/O. The actuation of the HIs is based on two different types of motor drivers. The control system kernel is based on RTOS which ensures high performances capabilities (up to 50KHz typical switching time with few microsecond latency). All the data I/O are managed by specific real-time device drivers. Connection with remote PC computer is based on UDP/IP protocol which ensures the required high data throughput with low latencies.

The system is controlled in order to replicate on the end-effector a desired value of force. In Figure 14 it is shown a generic scheme of the control system. The action of the human model in the loop has been modeled as a passive impedance Z_H which is directly coupled with the Haptic Interface.

The dynamics of the exoskeleton is described by the classical dynamic equation for multi-joint robots [10]:

$$B(\mathbf{q})\ddot{\mathbf{q}} + C(\mathbf{q}, \dot{\mathbf{q}})\dot{\mathbf{q}} + G(\mathbf{q}) = J^T \mathbf{h} \qquad (1)$$

where B is the Inertia matrix, C represents the Coriolis effects matrix, G contains the joint gravity torques and $\mathbf{h}$ is the generalized external forces vector[1]. All the mass data (i.e. mass, geometry, centre of gravity and inertia tensors for all the links) and all geometrical dimensions have been estimated by 3D CAD models. The high precision manufacturing process, allows to conclude that most of data derived from the CAD design are reliable.

When the system operates in force-feedback mode, it can generate a virtual kinematic constraint to the user's movements corresponding to the contact with a surface.

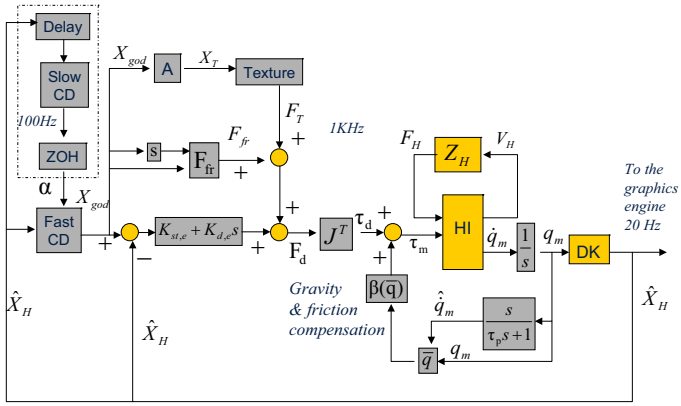

Figure 14. The control scheme.

The desired value of force is computed through the estimation of a desired position for the end effector called $\mathbf{X}_{god}$. The desired position is computed through a constraint-based algorithm, based on the god-object concept introduced in [7] and is sent as reference posi-

1 The vector than contains both force and torque applied by structure on external environment.

tion to the controller, that takes as input the error between $\mathbf{X}_{god}$ and the actual position $\mathbf{X}$.

The position of the end-effector $\hat{\mathbf{X}}$ is estimated through the Direct Kinematics (DK block) law from motor encoder readings. The $\mathbf{X}_{god}$ is generated by an haptic rendering algorithm that on the basis of the geometry simulated in the environment can calculate both collision and the amount of penetration inside the object. Additional terms are then added, $\mathbf{F}_{fr}$ and $\mathbf{F_T}$ to simulate surface properties of the object, based on local micro-geometry, such as friction and textures. Once that the desired value of force $\mathbf{F}_d$ has been computed:

$$\mathbf{F}_d = (K_{st,e} + K_{d,e}s)(\mathbf{X}_{god} - \hat{\mathbf{X}}) + \mathbf{F}_{fr} + \mathbf{F_T} \qquad (2)$$

a command torque is generated at motors to display this force at the end effector. A feedforward term $\beta(\overline{\mathbf{q}})$ is computed in order to compensate for friction and gravity errors. The computation of this feedforward term is based on a accurate model of the transmission system and of energy losses, according to the model presented in the previous section.

7.2. Experimental data

Figure 15 represents the forces measured at the end-effector, measured as a torque applied on the first joint, during the manipulation in free motion of the end-effector in the two conditions of active (blue) or non (red) friction compensation. In the latter case the motors provide only the static torque necessary to achieve the gravity compensation. It can be noticed how the active compensation of friction can reduce the effects of friction of more than 50%.

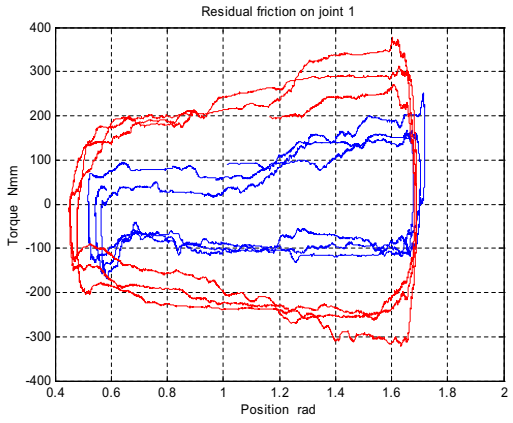

Figure 15. Comparison of force required to move the exoskeleton at the EF with and without active friction compensation

8. Conclusions

The mechanical design of a new arm exoskeleton for the human arm has been presented. The device can achieve a remarkable maximum force to weight ratio, close to 1, and presents reduced levels of friction and good transparency.

References

[1] M. Bergamasco, B. Allotta, L. Bosio, L. Ferretti, G. Parrini, G.M. Prisco, F. Salesdo, G. Sartini, "An Arm Exoskeleton System for Teleopera-tion and Virtual Environments Applications", IEEE Int.Conf.On Robotics and Automation, pp.1449-1454, 1994

[2] Sooyong Lee, Jangwook Lee, Woojin Chung, Munsang Kim, Chong-Won Lee, Mignon Park, "A new exoskeleton-type masterarm with force reflection :controller and integration", IEEE Int. Conf. on Intelligent Robots and Systems, Pages:1438 - 1443 vol.3, 1999

[3] N. Tsagarakis, D.G. Caldwell, G.A. Medrano-Cerda, "A 7 DOF pneumatic muscle actuator (pMA) powered exoskeleton" IEEE International Workshop on Robot and Human Interaction. RO-MAN '99. 8th, 27-29 Sept. 1999 Pages:327 - 333.

[4] M. Bergamasco, C.A. Avizzano, G. Di Pietro, F. Barbagli, A. Frisoli, "The museum of pure form: system architecture" 10th IEEE International Workshop on Robot and Human Interactive Communication, 18-21 Sept. 2001, Pages:112 - 117

[5] A. Frisoli, G.M. Prisco, F. Salsedo, M. Bergamasco, "A two degrees-of-freedom planar haptic interface with high kinematic isotropy" 8th IEEE International Workshop on Robot and Human Interaction, 27-29 Sept. 1999, Pages:297 - 302

[6] E. Papadopoulos, K. Vlachos, D. Mitropoulos, "Design of a 5-dof haptic simulator for urological operations" IEEE International Conference on Robotics and Automation, 11-15 May 2002, Pages:2079 - 2084 vol.2

[7] C.B. Zilles, J.K. Salisbury. 2A constraint-based god-object method for haptic display", Proceedings of IEEE IROS 1995.

[8] Immersion Corporation Web Site, Cybergrasp http://www.immersion.com

[9] N. Ando, P.T. Szemes, P. Korondi, H. Hashimoto, "Friction compensation for 6DOF Cartesian coordinate haptic interface" IEEE/RSJ International Conference on Intelligent Robots and System, 30 Sept.-5 Oct. 2002, Pages:2893 - 2898 vol.3

[10] L. Sciavicco, B. Siciliano, "Modeling and control of industrial manipulators", McGraw-Hill, 1995

[11] G.M. Prisco, M. Bergamasco, "Dynamic modelling of a class of tendon driven manipulators", 8th International Conference on Advanced Robotics, 7-9 July 1997, Pages:893 - 899

[12] Patent N. WO2004058458 "Exoskeleton Interface Apparatus", Salsedo F. , Dettori A. , Frisoli A., Rocchi F., Bergamasco M., Franceschini M.

[13] Patent N. WO2004058457 "Tendon-driven rotational joint for exoskeleton structure", Salsedo F., Dettori A., Bergamasco M.